

Shear Banding and Colloidal Models

Mikael Mohtaschemi¹, Anni Karppinen², Tapio Saarinen², Antti Puisto¹,
Arttu Lehtinen¹, Xavier Illa¹, Mikko Alava¹

¹Aalto University, School of Science, Department of Applied Physics,
P.O. Box 14100, FI-00076 AALTO, Finland

²Aalto University, School of Chemical Technology, Department of Biotechnology and
Chemical Technology, P.O. Box 16100, 00076 Aalto, Finland

ABSTRACT

We investigate the rheological behaviour of colloidal suspensions, a class of complex fluids, in the view of modeling microfibrillated cellulose rheology using the population balance equations, which are frequently used in this context. For spatially heterogeneous phenomena the model is further incorporated to a Couette rheometer setup discretized in the radial direction (1-D). We show here that many of the rheological features, complicating the standard rheological experiments of various complex fluids like yield stress behaviour, steady state shear banding as well as transient shear banding can be captured with this model.

INTRODUCTION

The potential resource savings and improved properties related to nanomaterials in composites^{1,2} have increased the interest of a wider audience towards microfibrillated cellulose (MFC)³. Several presently running large projects aim at the application of MFC in the paper and board industry. Moreover, other application prospects have appeared since the discovery of the peculiar, whilst tunable, rheological properties of MFC⁴, which are characterized by intense shear thinning. Application possibilities as a rheology modifier, for instance, in the food industry, requires further knowledge on the physical origins of such rheological behavior and its implica-

tions to the proper processing conditions.

Modeling the aspects of rheology of unstable colloids, such as MFC, has been a prolonged challenge in the scientific community. Presently, the way to simulate the aggregate size distribution at the continuum level is using the population balance equations (PBE). In the population balance equations an essential part of the underlying physics enters via the aggregation and fragmentation kernels, for example the kernel corresponding to aggregation induced by Brownian motion or laminar shear. The kernels are connected to the rheological features in line with what has been proposed so far^{5,6}. E.g. Brownian motion introduces aging effects and possible negative slopes in the constitutive equation and thus steady state shear banding. Many of the complex phenomena require an explicit shear rate dependency in at least one of the kernels.

The present paper is an attempt to understand qualitatively the complex phenomenology involved in the rheology of MFC through an *ab-initio* colloidal model taking into account the evolution of the internal structure of the colloid at the mean field level. The rest of the paper is organized such that: First, we will describe the experimental setup and results obtained for MFC. Then we will present an overview of the model. After that, the phenomenology observed in the simulations is explained. Finally, the conclusions will fin-

ish the paper.

EXPERIMENTS

Microfibrillated cellulose (MFC) was prepared from never dried birch pulp by mechanical disintegration in Supermasscolloider (Masuko Sangyo). Solid content of the material was 1% (w/w).

The measurements were performed using a dynamic rotational rheometer (AR G2, TA Instruments), with a standard metal concentric cylinders geometry (ISO 3219/DIN 53 019) and a peltier element temperature control. The bob and cup radii were 14 and 15 mm, respectively. Stepped flow measurements were measured from shear rate 500 s^{-1} to shear rate 10^{-3} s^{-1} using point times of 60, 6, and 1 s. Before each stepped flow measurement, the sample was sheared at 500 s^{-1} for 10 min. A point time 600 s was measured in similar manner but with a separate sample.

RESULTS

Fig. 1 shows the shear stress as a function of shear rate for 1% (w/w). MFC water suspension with different point times (the time that each shear rate was performed). At low shear rates, the shear stress was constant but heavily dependent on the point time. The shortest point time (1 s) gave shear stress $\sim 6 \text{ Pa}$, whereas the longest point time only (600 s) gave shear stress of $\sim 0.5 \text{ Pa}$. At high shear rates, the shear stress started to increase, and the difference between the point times reduced with the exception of the point time 1 s.

THE MODEL

As it is clear from the experiments of the previous section, the complex rheological behaviour of MFC water suspensions is dependent on time and shear rate and thus the usual simple approaches like explaining the flowcurve using empirical Herschel-Bulkley behavior can not be used. Instead, a more fundamental level description is needed. Here, as a first principles approach, the population balance equa-

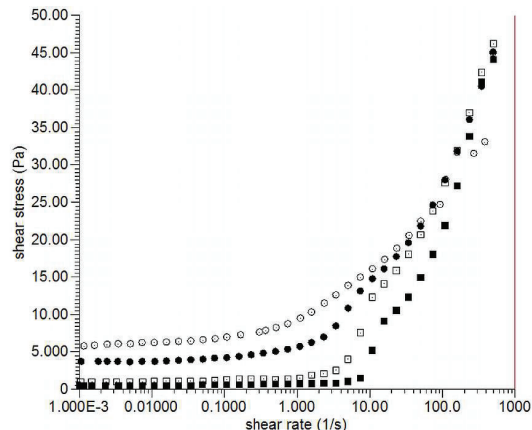


Figure 1: Shear stress as a function of shear rate for 1% (w/w) MFC suspension with varying point times: 1 s (\circ), 6 s (\bullet), 60 s (\square), and 600 s (\blacksquare).

tions are used to model the unstable colloidal suspension at the continuum level. The Schmolukowski⁷ equations, which for the number of aggregates containing i monomers reads

$$\frac{dn_i}{dt} = \frac{1}{2} \sum_{j=1}^{i-1} k^A(i-j, j)n_{i-j}n_j - \sum_{j=1}^{\infty} k^A(i, j)n_i n_j - k^B(i)n_i + \sum_{j=i+1}^{\infty} \beta(j, i)k^B(j)n_j \quad (1)$$

where k^A and k^B are the aggregation and fragmentation kernels, respectively. These equations essentially describe the time evolution of the aggregate size distribution.

In order for aggregation to take place, particles first have to approach one another. The main effects typically taken into account are sedimentation, Brownian motion and aggregation due to applied shear. In this paper only the collisions of Brownian like motion and laminar shear are considered. The collision rate due to Brownian motion is given by the following kernel⁸

$$\alpha_{i,j}^{Br} = \frac{2k_B T}{3\mu} \left(\frac{1}{r_i} + \frac{1}{r_j} \right) (r_i + r_j) \quad (2)$$

For the collision rate due to laminar shear the formula obtained by Camp and Stein⁹

is used

$$\alpha_{i,j}^{LS} = \frac{4}{3} \dot{\gamma} (r_i + r_j)^3. \quad (3)$$

In the above equations μ is the dynamic viscosity, r_i the radius of particles of size i , k_B is the Boltzmann constant, and $\dot{\gamma}$ the shear rate. Not all collisions lead necessarily to aggregation. This is taken into account by the collision efficiency C_e which is here taken to be a constant. Assuming the superposition principle for the collision rates, the aggregation kernel is thus given by

$$k^A(i, j) = C_e (\alpha_{i,j}^{Br} + \alpha_{i,j}^{LS}) \quad (4)$$

For the fragmentation a pre-formulated exponential kernel is used¹⁰. The aggregate size distribution is coupled to the local viscosity via the effective volume fraction ϕ ¹⁰.

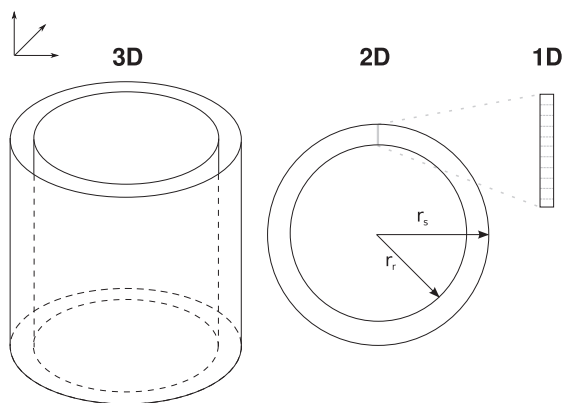


Figure 2: The discretization of the Couette.

For modeling spatial effects, expected to occur in the rheological experiments, the model as described above is implemented to a Couette geometry discretized in 1D in the radial direction (see Fig. 2). In particular at each grid cell a separate aggregate size distribution is evolved at the local shear rate. The local shear rate is given by¹¹

$$\dot{\gamma}(r) = \frac{\Omega_b - \Omega_a}{r^2 \mu(r) \int_{R_a}^{R_b} \frac{1}{r^3 \mu(r)} dr}, \quad (5)$$

where Ω_a (Ω_b) are the inner (outer) radial velocities, R_a (R_b) the inner (outer) radii of

the Couette and $\mu(r)$ the local viscosity with the corresponding ϕ .

To solve Eq. 1, it is discretized by the classes method of Kumar and Ramkrishna¹². The resulting model is solved numerically using the Adams-Moulton integration scheme as implemented in the SUNDIALS library package¹³.

PHENOMENA

With the PBE model as described above much of the behaviour of the MFC water suspensions¹⁰ can be captured. In addition one might introduce phenomena such as shear banding and compare the simulated results in a Couette with the experimental ones (Fig. 1). In particular the current spatial model has proven to provide a wide range of phenomena that can be captured and works thus as a tool to access an essential part of underlying physics of colloidal fluids. In this section an overview of the type of complex flow behaviour that have been successfully modeled is given and the resulting behaviour in a Couette device is addressed.

Yield stress behaviour can be obtained with an appropriate parameter setup. An example is shown in Fig. 3 (with $T=0$). Generally in the model, yield stress requires a high enough initial volume fraction and originates from the balance between the aggregation and fragmentation close to the maximum volume fraction. The yield stress fluid obtained in this way is a simple yield stress fluid without a critical shear rate. The steady state flow curve, shown in Fig. 3, changes gradually as shear rate independent aggregation term is included. (Here the Brownian like aggregation term is varied by changing the temperature T .) In particular one observes that at large shear rates the Brownian kernel has negligible impact on the flow curve. However, a negative slope in the flow curve at small shear rates is observed. In a rheometer context, this is indicative for the onset of steady state shear banding¹⁴.

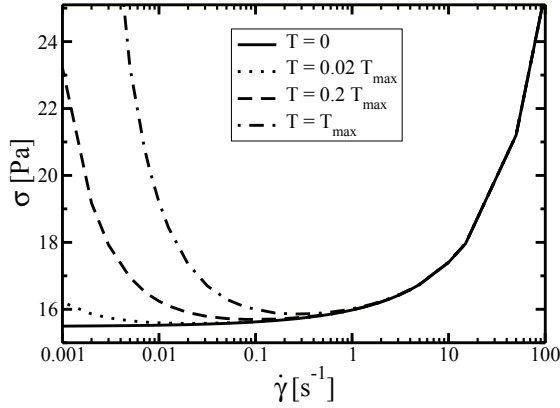


Figure 3: Evaluated constitutive flow curves with different amounts of Brownian-like aggregation.

In the Couette simulations, shear banding is indeed observed at steady state with sufficiently low imposed shear rates. This is demonstrated in Fig. 4. In this context shear localization is distinguished from a static shear band as, suggested in⁵, from the smooth transition between the flow and no flow parts in contrast with the discontinuous transition associated to the shear banding.

Observing the local shear rates and stresses in comparison to the constitutive flowcurve clearly demonstrates the existence of a critical shear rate. This is done in Fig. 5 for shear rate $\dot{\gamma} = 1 \text{ s}^{-1}$. As one can notice in the figure, all the points are along the corresponding constitutive flow curve (see also¹⁵). For the case with Brownian aggregation, only the points above the critical shear rate, which is here around 0.4 s^{-1} , are occupied. Shear rates below this value are not stable and the shear rate drops to zero as can be observed in Fig. 4. For the case without Brownian aggregation, all the shear rates are accessible and the transition from flow to no flow is continuous (shear localization). At sufficiently high shear rates no shear localization or shear banding is observed. Moreover, both the cases, Brownian and non-Brownian, give the same results. Obvi-

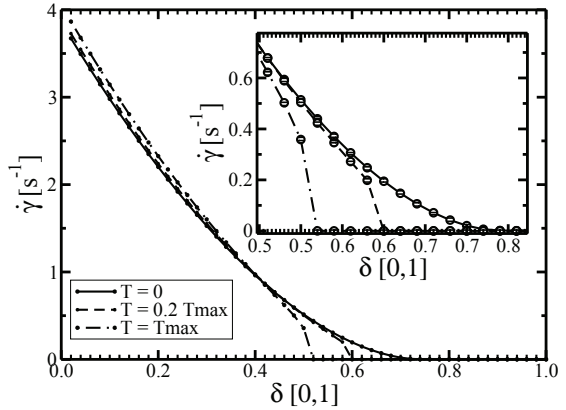


Figure 4: Local shear rate profile inside the Couette gap at steady state, at $\dot{\gamma} = 1 \text{ s}^{-1}$ with different amounts of Brownian aggregation. Without Brownian aggregation, shear localization at the rotor is observed, while with sufficient amount of Brownian aggregation a flowing band and a quiescent band is obtained. In the flowing part the lowest shear rate corresponds to the critical shear rate.

ously, also the range of the local shear rates in the gap gets narrower.

An interesting point is how the real flow curve of the colloid as shown in Fig. 3 compares to the flow curve as reported by a Couette rheometer. Here the stress is the one measured at the inner rotating cylinder and the applied shear rate is obtained, with the commonly used approximation of a Newtonian flow profile, from

$$\dot{\gamma}(R_a) = (\Omega_a - \Omega_b) \frac{R_b^2}{R_b^2 - R_a^2} \quad (6)$$

The flow curve, which would have been reported by the Couette device together with the real flow curve at low shear rates are shown in Fig. 6 for three cases with different amounts of Brownian like aggregation. In the figure one can observe that a Couette device would report quite similar results for all three cases and in particular does not capture any negative slope.

It should be noticed that the set of parameters used here are not fitted to

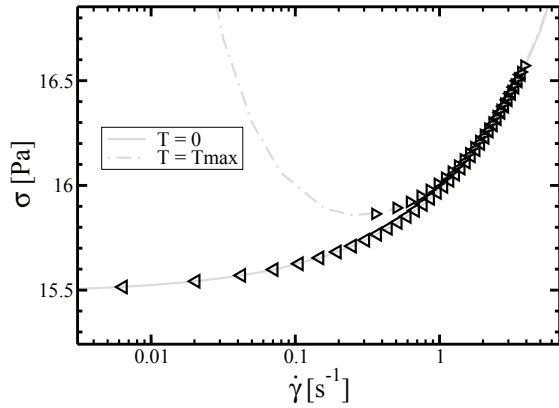


Figure 5: \triangleleft and \triangleright local shear rate and stress values at $\dot{\gamma} = 1 \text{ s}^{-1}$ and the corresponding constitutive curves.

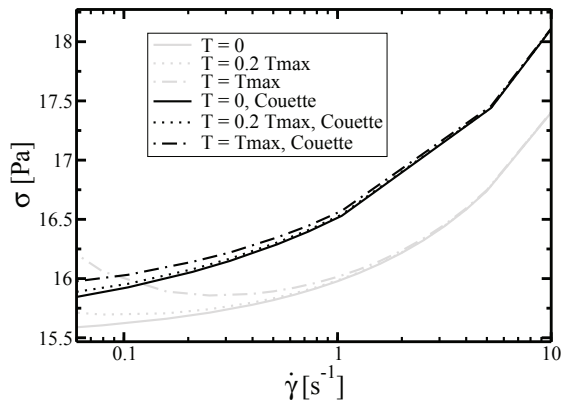


Figure 6: Steady state flow curve as reported by the Couette device compared to the real underlying constitutive curves.

real world fluids and thus do probably not represent a physically meaningful set. For completeness the used parameters are given in the Table 1.

CONCLUSIONS

A population balance based rheological model was implemented and studied in the context of modeling rheological measurements of colloidal suspensions, more specifically, MFC. This was done hoping to understand the related phenomenology and to help the interpretation of the related experimental data. The model showed thixotropy in both of its definitions⁵: time

Table 1: The used parameters for running the simulations.

Parameter	Value
R_a	0.0239 m
R_b	0.025 m
d_f	2.1
F_b	5.1e-10 N
C_e	0.02
r_0	1.0e-6 m
ϕ (fully dispersed)	0.62

dependence of the viscosity, and associated critical shear rate. While not addressed in this paper, different transient effects such as those during step changes in shear rate¹⁶, typical for flow curve measurements, can be addressed in great detail with a model setup as exploited here.

Microfibrillated cellulose being formed of small particles with the typical lengths below few μm and wide length distributions, is demonstrated in this paper to show thixotropy, the time dependence of the viscosity. The other aspect of thixotropy, the critical shear rate, can not be addressed in the experiments without measuring the local velocity profiles. Based on the modeling, however, these two features are shown not to be inherently linked: in principle, one could have time dependent viscosity without having a critical shear rate. Therefore, to further continue the modeling work, spatially resolved experiments measuring the local velocity profiles should be performed for MFC.

Moreover, the time dependence in the MFC flow curve can rise at least from two interlinked issues. First, the material can behave time dependently such that it relaxes homogeneously in the gap without shear banding. Second, the material can develop shear bands, and the shear band edge can move in time. Both evolutions produce basically similar experimental result in a rheometer. However, in the first case the result is truly a material response, and in the second case it is an experimental artifact resulting from the negative slope

in the intrinsic flow curve. As mentioned before, these two processes are somewhat interlinked in the sense that if the relaxation rate of the viscosity is dependent on the shear rate, then the first process implies the second one if the stress is not completely homogeneous over the gap(, which it never is).

ACKNOWLEDGEMENTS

This work was supported by the Effnet program in the Finnish Forest Cluster Ltd, and EU framework 7 program SUNPAP. Also, the support from the Academy of Finland through the COMP center of excellence, the project number 140268 and within the framework of the International Doctoral Programme in Bioproducts Technology (PaPSaT) are acknowledged.

REFERENCES

- Hubbe, M.A., Rojas, O.J., Lucia, L.A., and Sain, M. (2008). "Cellulosic nanocomposites: A review". *BioRes.*, **3**, 929.
- Siró, I. and Plackett, D. (2010). "Microfibrillated cellulose and new nanocomposite materials: a review". *Cellulose*, **17**, 459. doi: 10.1007/s10570-010-9405-y.
- Zimmermann, T., Pöhler, E., and Geiger, T. (2004). "Cellulose Fibrils for Polymer Reinforcement". *Adv. Eng. Mat.*, **6**, 754.
- Pääkkö, M., Ankerfors, M., Kosonen, H., Nykänen, A., Ahola, S., Österberg, M., Ruokolainen, J., Laine, J., Larsson, P., Ikkala, O., and Lindström, T. (2007). "Enzymatic Hydrolysis combined with mechanical shearing and high-pressure homogenization for nanoscale cellulose fibrils and strong gels". *BioMacromol.*, **8**, 1934.
- Møller, P.C.F., Mewis, J., and Bonn, D. (2006). "Yield stress and thixotropy: on the difficulty of measuring yield stresses in practice". *Soft Matter*, **2**, 274.
- Fielding, S. (2007). "Complex dynamics of shear banded flows". *Soft Matter*, **3**, 1262–1279.
- von Smoluchowski, M. (1917). "Versuch einer mathematischen Theorie der Koagulationskinetik kolloider Lösung". *Z. Phys. Chem*, **92**, 129.
- Runkana, V. and Somasundaran, P. (2004). "Mathematical modeling of polymer-induced flocculation by charge neutralization". *J. Colloid Interface Sci.*, **270**, 347.
- Camp, T. and Stein, P. (1943). "Velocity gradients and internal work in fluid motion". *Journal of the Boston Society of Civil Engineers*, **30**, 219–237.
- Puisto, A., Illa, X., Mohtaschemi, M., and Alava, M. (2012). "Modeling the viscosity and aggregation of suspensions of highly anisotropic nanoparticles". *Eur. Phys. J. E*, **35**, 6.
- Phillips, R.J., Armstrong, R.C., Brown, R.A., Graham, A.L., and Abbott, J.R. (1992). "A constitutive equation for concentrated suspensions that accounts for shear induced particle migration". *Phys. Fluids A*, **4**, 30.
- Kumar, S. and Ramkrishna, D. (1996). "On the solution of population balance equations by discretization—I. A fixed pivot technique". *Chem. Eng. Sci.*, **51**, 1311.
- Cohen, S.D. and Hindmarsh, A.C. (1996). "CVODE, A stiff/nonstiff ode solver in C". *Comp. Phys.*, **10**, 138.
- Adams, J.M., Fielding, S.M., and Olmsted, P.D. (2011). "Transient shear banding in entangled polymers: A study using the Rolie-Poly model". *J. Rheol.*, **55**, 1007.
- Divoux, T., Tamarii, D., Barentin, C., and Manneville, S. (2011). "Fluidization dynamics of a simple yield stress fluid: a long way from transient shear banding to steady state". *Arxiv preprint arXiv:1110.1786*.
- Mohtaschemi, M., Puisto, A., Lehtinen, A., Illa, X., and Alava, M.J. "Modeling transient shear banding in colloidal suspensions". *In preparation*.